A tractable example of perturbation theory with a field cutoff: the anharmonic oscillator

2005 J. Phys. A: Math. Gen. 38 8139

(http://iopscience.iop.org/0305-4470/38/37/013)

INSTITUTE OF PHYSICS PUBLISHING JOURNAL OF PHYSICS A: MATHEMATICAL AND GENERAL

J. Phys. A: Math. Gen. **38** (2005) 8139–8153 doi:10.1088/0305-4470/38/37/013

A tractable example of perturbation theory with a field cutoff: the anharmonic oscillator

L Li[1] **and Y Meurice**[1,2,3]

[1] Department of Physics and Astronomy, The University of Iowa, Iowa City, IA 52242, USA
[2] Kavli Institute for Theoretical Physics, Santa Barbara, Santa Barbara, CA 93106, USA

E-mail: yannick-meurice@uiowa.edu

Received 3 June 2005, in final form 25 July 2005
Published 31 August 2005
Online at stacks.iop.org/JPhysA/38/8139

Abstract

For $\lambda\phi^4$ models, the introduction of a large field cutoff improves significantly the accuracy that can be reached with perturbative series but the calculation of the modified coefficients remains a challenging problem. We show that this problem can be solved numerically, and analytically in the limits of large and small field cutoffs, for the ground-state energy of the anharmonic oscillator. For the two lowest orders in λ, the approximate formulae obtained in the large field cutoff limit extend unexpectedly far in the low field cutoff region and there is a significant overlap with the small field cutoff approximation. For the higher orders, this is not the case; however the shape of the transition between the small field cutoff regime and the large field cutoff regime is approximately order independent.

PACS numbers: 11.15.Bt, 12.38.Cy, 31.15.Md

1. Introduction

Perturbative methods and Feynman diagrams have played an important role in the development of quantum field theory and its applications. However, perturbative series usually have a zero radius of convergence [1]. For scalar models with $\lambda\phi^4$ interactions, the coefficients of perturbative series grow factorially. For any fixed, strictly positive, value of λ there exists an order beyond which adding higher order terms diminishes the accuracy. This feature will restrict our ability to perform high precision tests of the standard model (for instance, $g-2$ of leptons and the hadronic width of the Z^0) during the next decades.

The large order behaviour of the series is dominated by large field configurations which have little effect on low energy observables. Introducing a large field cutoff [2, 3] in the path integral formulation of scalar field theory dramatically improves the large order behaviour

[3] Also at the Obermann Center for Advanced Study, University of Iowa, USA.

of the perturbative series. In two non-trivial examples [3], this procedure yields series that have finite radii of convergence and tend to values that are exponentially close to the exact ones. This also allows us to define the theory for negative or complex values of λ, a subject that has raised a lot of interest recently [4, 5]. An important feature of this approach is that for a perturbative expansion at a given order in λ, it is possible in some cases to determine an optimal field cutoff using the strong coupling expansion [6, 7], bridging the gap between the two expansions. In other words, the modified perturbative methods allow us to take into account non-perturbative effects.

Despite these promising features, calculating the modified coefficients remains a challenging technical problem. While developing a new perturbative method (see, e.g., [8, 9] for the δ expansion), it is customary to demonstrate the advantages of a method with simple integrals and the non-trivial, but well-studied [10, 1], case of the anharmonic oscillator. A simple integral has been discussed in [6]. In this paper, we show not only that this programme can be completed in the case of the anharmonic oscillator, but also that the results show remarkable properties:

- For the two lowest orders, the approximate formulae obtained in the large field cutoff limit extend unexpectedly far in the low field cutoff region.
- For the higher orders, the transition between the small field cutoff regime and the large field cutoff regime can be approximately described in terms of a single function.

The results are presented in the following way. In section 2, we define the model considered and the numerical calculation of the modified coefficients. In section 3, we discuss the radius of convergence of the modified series from a numerical point of view. In sections 4 and 5, we present the approximate methods at small and large field cutoff. Rigorous bounds on the radius of convergence of series encountered in the previous sections are given in section 6. The question of the interpolation between the small and large field cutoff regimes is discussed in section 7. The importance of a complete understanding of this question, as well as the extension to field theory is discussed in the conclusions.

2. The problem and its numerical solution

In this section, we introduce the anharmonic oscillator with a 'field cutoff' and we explain how to calculate numerically the perturbative series in the anharmonic coupling λ. This method was first used in [3] and tested with the known results [10] up to order 20. It is a perturbative version of the numerical method proposed in [11]. For convenience, we use quantum mechanical notation instead of field theoretical ones $\phi \to x, m \to \omega$ and the field cutoff will be denoted $x_{\max}$. We also use units such that $\hbar = 1$ and the 'mechanical mass' m is 1. However, the harmonic angular frequency ω, will sometimes be used as an expansion parameter and will be kept arbitrary in the equations. In these units, $x_{\max}\sqrt{\omega}$ and λ/ω^3 are dimensionless. The Hamiltonian reads

$$H = \frac{p^2}{2} + V(x) \tag{1}$$

with

$$V(x) = \begin{cases} \frac{1}{2}\omega^2 x^2 + \lambda x^4 & \text{if } |x| < x_{\max} \\ \infty & \text{if } |x| \geqslant x_{\max}. \end{cases} \tag{2}$$

Our main goal is the calculation of the modified coefficients $E_0^{(k)}(\sqrt{\omega}x_{\max})$ of the perturbative series for the ground-state energy:

$$E_0(x_{\max},\omega,\lambda)=\omega\sum_{k=0}^{\infty}E_0^{(k)}(\sqrt{\omega}x_{\max})\times(\lambda/\omega^3)^k. \tag{3}$$

For this purpose, we will solve perturbatively the time-independent Schrödinger equation with the boundary condition $\Psi(x_{\max})=0$. We proceed as in [11]. Setting

$$\Psi(x)\propto\exp\left(-\int_{x_0}^{x}\mathrm{d}y(L(y)/K(y))\right), \tag{4}$$

the Schrödinger equation reads

$$L'+2(V-E)K+GL=0 \tag{5}$$

$$K'+L+GK=0 \tag{6}$$

where $G(x)$ is an arbitrary function. The second of these equations implies that

$$\Psi(x)\propto K(x)\,\mathrm{e}^{\int^x\mathrm{d}yG(y)}. \tag{7}$$

It is possible to show [11] that if G and V are polynomials:

- equations (5), (6) can be solved by power series which define entire functions; recursion formulae and initial conditions (different for even and odd solutions) are given in [11],
- the zeros of Ψ are the same as the zeros of K.

This implies that the energy levels can be obtained by solving

$$K(x_{\max},\omega,\lambda,E)=0 \tag{8}$$

for the variable E, and that polynomial approximations can be used for this purpose. We now use the perturbative expansion

$$E=\omega\sum_{k=0}^{\infty}E^{(k)}(\lambda/\omega^3)^k. \tag{9}$$

We assume that $\omega>0$. The case $\omega=0$ is simpler and will be discussed in section 5. By construction, the coefficients $E^{(k)}$ are dimensionless and can only depend on $\sqrt{\omega}x_{\max}$ when their value is fixed using equation (8). In the following, this dependence will sometimes be kept implicit in order to reduce the size of some equations. We also recall that if we had not chosen the units $\hbar=m=1$, the dimensionless quantities used above would read $(\sqrt{\omega m/\hbar}x_{\max})$ and $\hbar\lambda/m^2\omega^3$.

We need to set the expansion

$$K(x_{\max},\omega,\lambda,E)=K^{(0)}(\sqrt{\omega}x_{\max},E^{(0)})+ \tag{10}$$

$$(\lambda/\omega^3)K^{(1)}(\sqrt{\omega}x_{\max},E^{(0)},E^{(1)})+\cdots \tag{11}$$

equal to zero order by order in λ. We can approximate the $K^{(k)}$ by polynomials. We then start by solving $K^{(0)}(\sqrt{\omega}x_{\max},E^{(0)})=0$ for $E^{(0)}$ using Newton's method. This corresponds to the problem of an harmonic oscillator potential that becomes infinite at $x=\pm x_{\max}$. The various zeros of the polynomial correspond to the (even or odd depending on how we construct K [11]) spectrum of this model. The ground-state energy is obtained by taking the lowest even solution. By increasing the degree of the polynomial approximation, we can stabilize the numerical value with great accuracy. The independence on G of the exact equations, before we use polynomial approximations, can be used to test the numerical accuracy of the polynomial approximations used for K. In practice a good choice is made by having K of order 1 for E

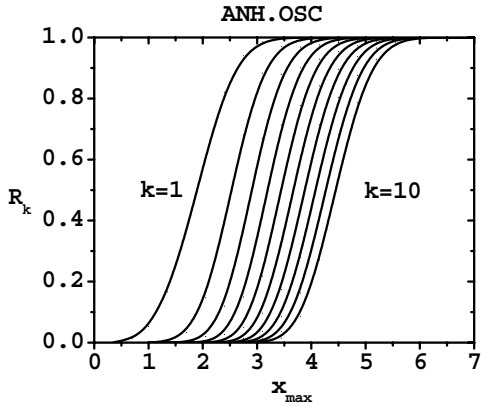

Figure 1. The numerical values of $R_k(x_{\max})$ for $k = 1, \ldots, 10$ and $\omega = 1$.

close, but not fine tuned, to its actual value. Since the potential is even, it is natural to have K even and G and L odd, however we noted that introducing a small parity breaking in G usually improves the numerical stability. We then solve $K^{(1)}(x_{\max}, E^{(0)}, E^{(1)}) = 0$ for $E^{(1)}$. Since $E^{(1)}$ appears only linearly in the order λ expansion of K, it is a linear equation for this quantity and can be solved trivially. The same reasoning shows that the higher order equations are linear in $E^{(k)}$.

By using this method, we have calculated the first ten coefficients for $\omega = 1$ and values of $x_{\max}$ between 0.5 and 7. In order to allow a comparison among the different orders, we define the ratios

$$R_k(\sqrt{\omega}x_{\max}) \equiv E_0^{(k)}(\sqrt{\omega}x_{\max}) \Big/ E_0^{(k)}(\infty), \tag{12}$$

which all tend to 1 in the $x_{\max} \to \infty$ limit and to 0 in the $x_{\max} \to 0$ limit. The numerical values of these ratios are shown in figure 1. A striking feature is that the curves for the various orders have approximately the same shape and that we could approximately superpose them by appropriate horizontal translations. Before studying these curves in the large and small $x_{\max}$ limits, we will discuss numerical estimates for the radius of convergence of the modified series that can be extracted from these data.

3. Numerical evidence for a finite radius of convergence

If we calculate the integral of a function defined by a series which is uniformly convergent over the range of integration, it is legitimate to interchange the sum and the integral. On general grounds, one would thus expect that if we calculate the partition function of a properly regularized theory (say on a finite lattice) with a field cutoff, the perturbative expansion becomes convergent for arbitrary complex values of the coupling. The ground-state energy of the anharmonic oscillator can be obtained from the logarithm of the partition function and consequently, we would expect that its perturbative expansion will have a finite radius of convergence. This radius will depend on the position of the complex zeros of the partition function.

It is sometimes possible to estimate the radius of convergence by considering the empirical asymptotic behaviour of the perturbative series. However, with a limited series, transient behaviour is often encountered. It is clear from figure 1 that if $x_{\max}$ is large enough, the beginning of the series looks like its $x_{\max} \to \infty$ limit which grows at a factorial rate.

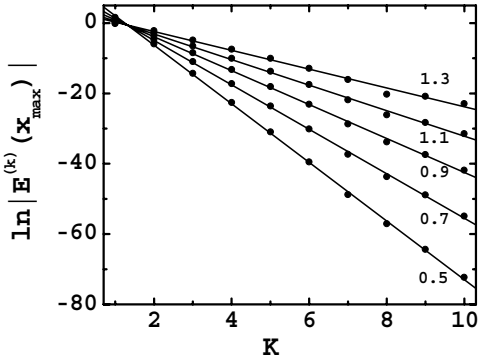

Figure 2. $\ln|E_0^{(k)}(x_{\max})|$ versus k for $x_{\max} = 0.5, 0.7, \ldots, 1.3$ (from bottom to top); ω was set to 1.

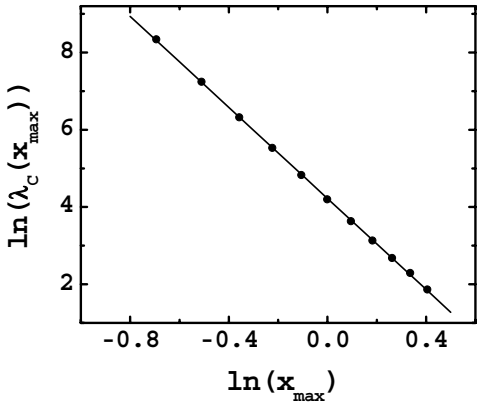

Figure 3. $\ln \lambda_c(x_{\max})$ versus $\ln x_{\max}$ for $\omega = 1$. The line is $4.22 - 5.89x$.

Consequently, in order to attempt to probe the asymptotic behaviour, we will only consider $x_{\max}$ such that the available coefficients are significantly smaller than their value when $x_{\max}$ is infinite. For this reason, we have limited the range of investigation to $x_{\max} < 1.3$. If we have a finite radius of convergence λ_c, we expect that for k sufficiently large, the kth coefficient grows like the kth power of a number which depends on $\sqrt{\omega}x_{\max}$ only and that we will denote $P(\sqrt{\omega}x_{\max})$:

$$\left|E_0^{(k)}(\sqrt{\omega}x_{\max})\right| \propto (P(\sqrt{\omega}x_{\max}))^k. \tag{13}$$

When this is the case, $\lambda_c(x_{\max}, \omega) = \omega^3/P(\sqrt{\omega}x_{\max})$. In figure 2, we have plotted $\ln\left|E_0^{(k)}(\sqrt{\omega}x_{\max})\right|$ versus k. We see a clear linear behaviour and the slope can be interpreted as $\ln P(\sqrt{\omega}x_{\max})$. We can then study $\lambda_c(x_{\max}, \omega)$ as a function of $x_{\max}$. This is done in figure 3 where a log–log plot shows a clear linear behaviour. The slope is near 5.9 which is close to the value 6 that, we will argue in section 6, should hold in the limit of small $x_{\max}$ (see equation (40)). We conclude that in this limit, our numerical data suggest

$$\lambda_c(x_{\max}, \omega = 1) \simeq 65 \times x_{\max}^{-6}. \tag{14}$$

4. The large $x_{\max}$ limit

In this section, we first discuss the harmonic energy spectrum with vanishing boundary conditions at $\pm x_{\max}$ and then treat the anharmonic interactions with the usual perturbative methods. We work in the limit where $x_{\max}$ is large. This means that if we consider the nth energy level, $x_{\max}$ should be much larger than the largest zero of $H_n(x\sqrt{\omega})$. According to equation (6.32.5) of [12], this imposes the restriction $x_{\max} \gg \sqrt{2n/\omega}$ for large n. When all the zeros of H_n are well within $[-x_{\max}, x_{\max}]$, the new boundary conditions require changes that are exponentially small. It is clear that for any fixed $x_{\max}$, this condition will be violated for n sufficiently large.

4.1. The harmonic case

We first need to calculate the energy eigenvalues at $\lambda = 0$, $E_n^{(0)}(\sqrt{\omega}x_{\max})$, and their corresponding wavefunctions $\Psi_n^{(0)}(x)$. The wavefunction always depends on $x_{\max}$, but this will be kept implicit. We impose the boundary conditions $\Psi_n^{(0)'}(0) = 0$ for n even, $\Psi_n^{(0)}(0) = 0$ for n odd and $\Psi^{(0)}(x_{\max}) = 0$ in both cases. We will not pay attention to the overall normalization until the end of the calculation. When $x_{\max} \to \infty$, we have $E_n^{(0)}(\sqrt{\omega}x_{\max}) \simeq (n + 1/2)$ and we will use

$$\epsilon_n(\sqrt{\omega}x_{\max}) \equiv E_n^{(0)}(\sqrt{\omega}x_{\max}) - n - 1/2 \tag{15}$$

as our expansion parameter. Again, ϵ_n is a dimensionless quantity that can only depend on $\sqrt{\omega}x_{\max}$ and we will often keep this dependence implicit. We write

$$\Psi_n^{(0)}(x) \equiv K_n^{(0)}(x)\, \mathrm{e}^{-\omega x^2/2}. \tag{16}$$

This corresponds to a choice $G = -\omega x$ in equations (5)–(6) and consequently

$$-(1/2)K_n^{(0)\prime\prime} + \omega x K_n^{(0)\prime} - n\omega K_n^{(0)} = \epsilon_n \omega K_n^{(0)}. \tag{17}$$

We then expand

$$K_n^{(0)} = K_n^{(0)(0)} + \epsilon_n K_n^{(0)(1)} + \cdots. \tag{18}$$

When $x_{\max} \to \infty$, $\epsilon_n \to 0$, and we want to recover the usual harmonic oscillator solution. Consequently, we set $K_n^{(0)(0)}(x) = H_n(\sqrt{\omega}x)$, the nth Hermite polynomial which is obviously a solution of equation (17) at order 0 in ϵ_n. At order ϵ_n, we have

$$-(1/2)K_n^{(0)(1)\prime\prime} + \omega x K_n^{(0)(1)\prime} - n\omega K_n^{(0)(1)} = \omega H_n(\sqrt{\omega}x), \tag{19}$$

with the boundary conditions

$$K_n^{(0)(1)}(0) = K_n^{(0)(1)\prime}(0) = 0. \tag{20}$$

Remarkably, this inhomogeneous equation can be integrated exactly in two steps. First, we set

$$K_n^{(0)(1)}(x) = H_n(\sqrt{\omega}x)G_n(x). \tag{21}$$

This removes the explicitly n-dependent term and the equation depends only on G':

$$-(1/2)H_n(\sqrt{\omega}x)G_n'' + [\omega x H_n(\sqrt{\omega}x) - H_n'(\sqrt{\omega}x)\sqrt{\omega}]G_n' = \omega H_n(\sqrt{\omega}x). \tag{22}$$

We then write $G'(x) = N(x)\,\mathrm{e}^{\omega x^2}$ which removes the term linear in x and allows us to write the lhs as a total derivative. The solution is then

$$G_n(x) = -2\omega \int_0^x \mathrm{d}y (H_n(\sqrt{\omega}y))^{-2}\, \mathrm{e}^{\omega y^2} \int_0^y \mathrm{d}z\, \mathrm{e}^{-\omega z^2} (H_n(\sqrt{\omega}z))^2. \tag{23}$$

One can check that the lower bounds of integration imply the boundary conditions of equation (20). This is obvious when n is even. When n is odd, the z integral is of order y^3 when $y \to 0$ which overcompensates the y^{-2} of the other factors. Note that $G_n(x)$ is independent of $x_{\max}$. The integrand of the y integral has a double pole at the zeros of H_n, however it has no single pole. This can be seen by plugging a Laurent expansion of G' with poles of order 1 and 2 about a zero of H_n, and using the relation between the first and the second derivative of H_n at this zero provided by the defining equation for Hermite polynomials. This forces the coefficient of the simple pole to be zero. Consequently, when we express G as the integral of G', we can go around the double pole either above or below the real line and obtain the same result. In other words, we can regularize the y integral by replacing $(H_n(\sqrt{\omega}y))^{-2}$ by $(H_n(\sqrt{\omega}y) \pm \mathrm{i}\epsilon)^{-2}$. From these considerations, we see that $G(x)$ develops a simple pole when x approaches a zero of H_n, which compensate the simple zero of H_n. Due to the absence of single pole in G', there is no logarithmic singularity in G.

ϵ_n can be calculated by imposing the condition that the wavefunction vanishes at $x_{\max}$. This translates into the simple equation

$$\epsilon_n(\sqrt{\omega}x_{\max}) = -1/G_n(x_{\max}). \tag{24}$$

As ϵ_n increases, the non-trivial zeros of the wavefunction move towards the origin. The shift of these zeros is approximately linear in ϵ_n for large $x_{\max}$. For instance, for $n = 2$, the shift of the non-trivial zero $x_{(0)}$ obeys the approximate linear relation $\Delta x_{(0)} \simeq -0.145\epsilon_2$.

We now discuss in more detail the case of the ground state ($n = 0$). It should be noted that in this case the double integral can be expressed [13] in terms of generalized hypergeometric series

$$\begin{aligned} G_0(x) &= -\omega x^2 {}_2F_2(1, 1; 2, 3/2; \omega x^2) \\ &= -\frac{\sqrt{\pi}}{2} \sum_{k=1}^{\infty} \frac{(\omega x^2)^k}{k\Gamma(k + 1/2)}. \end{aligned} \tag{25}$$

This series defines a function that converges over the entire complex plane. The asymptotic form of $G_0(x_{\max})$, for $x_{\max}$ large, can be worked out by noting that the integral over y in equation (23) comes mostly from the region $y \simeq x_{\max}$ and consequently, we can extend the integral over z to infinity with exponentially small errors. The integral over y can then be approximately performed by expanding the argument of the exponential about $x_{\max}$. Using equation (24), we conclude that asymptotically

$$\epsilon_0(\sqrt{\omega}x_{\max}) \simeq 2\sqrt{\frac{\omega}{\pi}} x_{\max}\, \mathrm{e}^{-\omega x_{\max}^2}. \tag{26}$$

This result coincides exactly with the semi-classical estimate given in [11]. The validity of equation (26) can be checked numerically. For instance, for $x_{\max} = 7$ and $\omega = 1$, we get $\epsilon_0 = 4.14 \times 10^{-21}$ from equation (26) which agrees well with 4.10×10^{-21} obtained numerically.

In figure 4, we have plotted the asymptotic form equation (26) but also the full integral form

$$\epsilon_0(\sqrt{\omega}x_{\max}) = 1 \Big/ \left(2\omega \int_0^{x_{\max}} \mathrm{d}y\, \mathrm{e}^{\omega y^2} \int_0^{y} \mathrm{d}z\, \mathrm{e}^{-\omega z^2} \right). \tag{27}$$

One notes that the integral form stays accurate to much lower values of $x_{\max}$, even at very low values of $x_{\max}$, where it has no reason to be accurate, it gives a reasonable answer. This observation will be discussed further in section 7.

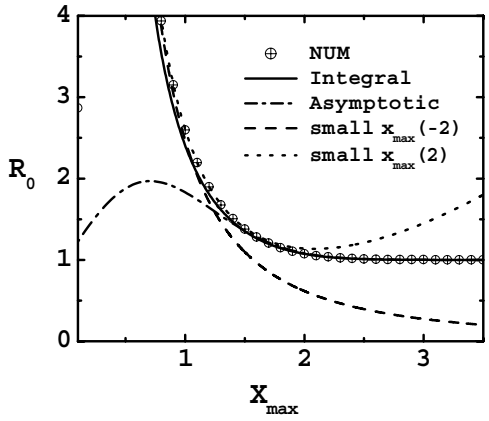

Figure 4. Numerical values of $R_0(x_{\max})$ (crossed circles) for $\omega = 1$, the integral formula of equation (27) (solid line), the asymptotic equation (26) (dash-dot line), the leading term ($\propto x_{\max}^{-2}$, dash line) of the small $x_{\max}$ expansion studied in section 5 and together with the $x_{\max}^2$ correction (dots). For $x_{\max} > 1.5$, the integral formula, its asymptotic form and the data are undistinguishable with the eye.

4.2. Anharmonic corrections

Having solved the problem for $\lambda = 0$ at first order in ϵ_n, we can use the usual methods of perturbation theory. $E_0^{(1)}$ can be calculated by taking the average of x^4 with the corrected ground state wavefunction constructed above:

$$E_0^{(1)} = \omega^2 N^{-1} \int_0^{x_{\max}} \mathrm{d}x \left|\Psi_0^{(0)}(x)\right|^2 x^4 \tag{28}$$

with the normalization constant

$$N = \int_0^{x_{\max}} \mathrm{d}x \left|\Psi_0^{(0)}(x)\right|^2. \tag{29}$$

Proceeding as for equation (26), we obtain in leading order

$$E^{(1)} \simeq (3/4) - \pi^{1/2}\omega^{5/2} x_{\max}^5 \, \mathrm{e}^{-\omega x_{\max}^2}. \tag{30}$$

Note that in this calculation, we have replaced $G_0(x)$ in the integral by its asymptotic form ($\propto x^{-1}\,\mathrm{e}^{\omega x^2}$ see equations (24)–(26)). The exponentials exactly cancel inside the integral and we are left with the integration of x^4/x. This is justified by the fact that most of the contributions come from the large x region. The validity of equation (30) can be checked numerically. For instance, for $x_{\max} = 7$ and $\omega = 1$, equation (30) gives a correction -4.97×10^{-18} while numerically we obtain -5.01×10^{-18}.

The good accuracy of equation (30) is shown in figure 5. In this figure, we also show the full integral formula of equation (28), where the integral was done numerically using the square of the order ϵ approximation for the ground state wavefunction, without discarding order ϵ^2 terms in the square. Again the integral formula stays valid at unexpectedly low values of $x_{\max}$. This will be explained in section 7.

The derivation of equation (30) is quite simple: ϵ_0 gives a contribution proportional to $x_{\max}\,\mathrm{e}^{-\omega x_{\max}^2}$ and the x-integral gives a factor $x_{\max}^4$. We conjecture that at leading order, a similar situation is encountered for higher order terms, and that

$$1 - R_k(\sqrt{\omega} x_{\max}) \propto x_{\max}^{4k+1}\,\mathrm{e}^{-\omega x_{\max}^2}. \tag{31}$$

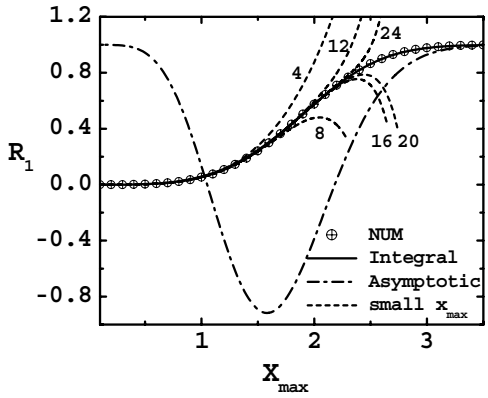

Figure 5. Numerical values of $R_1(x_{\max})$ (crossed circles) for $\omega = 1$, the integral formula of equation (28) (solid line), the asymptotic equation (30) (dash-dot line), the small $x_{\max}$ expansion studied in section 5 truncated at order $4, 8, \ldots, 24$ (dots). Series analysis suggests that the small $x_{\max}$ expansion converges for $x_{\max} < 2.9$.

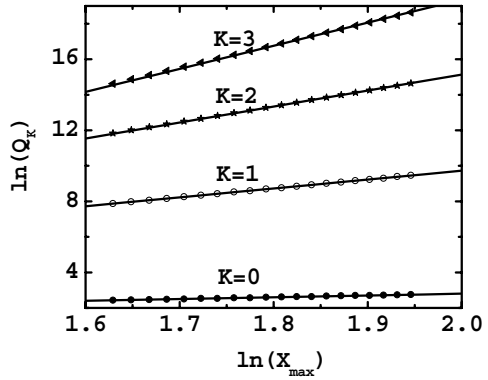

Figure 6. $\ln(Q_k(x_{\max}))$ versus $\ln(x_{\max})$ for $\omega = 1$. The explanations about the solid lines are given in the text.

For this purpose we have studied numerically the quantity

$$Q_k(\sqrt{\omega}x_{\max}) \equiv \mathrm{e}^{+\omega x_{\max}^2}(1 - R_k(\sqrt{\omega}x_{\max})), \tag{32}$$

which according to the conjecture should scale like $x_{\max}^{4k+1}$. In figure 6, we have set $\omega = 1$ and displayed $\ln(Q_k(x_{\max}))$ versus $\ln(x_{\max})$. The solid lines represent the linear functions $A_k + (4k+1)\ln(x_{\max})$. The constants A_k have been fitted using the last ten data points. Their numerical values are $A_0 = 0.802$ which compare well with the prediction of equation (26) $\ln(4\pi^{-1/2}) \simeq 0.814$, and $A_1 = -0.276$ which compares well with the prediction of equation (30) $\ln(4\pi^{-1/2}/3) \simeq -0.285$. The linear behaviour of the higher orders supports the conjecture.

5. The small $x_{\max}$ limit

When the field cutoff $x_{\max} \to 0$, the potential term in the harmonic oscillator is much smaller than the kinetic term, and in first approximation we can use the free particle in a box of

Table 1. The coefficients $E_0^{(k,l)}$.

$k\,l$:	0	1	2	3
0	1.234	6.535×10^{-2}	-5.923×10^{-4}	6.097×10^{-6}
1	4.110×10^{-2}	-1.169×10^{-3}	2.150×10^{-5}	-2.443×10^{-7}
2	-6.110×10^{-4}	2.555×10^{-5}	-5.079×10^{-7}	3.575×10^{-9}
3	1.020×10^{-5}	-4.571×10^{-7}	6.983×10^{-9}	9.506×10^{-11}
4	-1.517×10^{-7}	5.804×10^{-9}	2.492×10^{-11}	-7.641×10^{-12}

length $2x_{\max}$. The energy levels diverge as $x_{\max}^{-2}$ and it is convenient to introduce the following rescalings:

$$\tilde{H} = x_{\max}^2 H \qquad \tilde{x} = x/x_{\max} \qquad \tilde{\omega} = \omega x_{\max}^2 \qquad \tilde{\lambda} = \lambda x_{\max}^6.$$

We then obtain a new Hamiltonian

$$\tilde{H} = -\frac{1}{2}\left(\frac{\mathrm{d}}{\mathrm{d}\tilde{x}}\right)^2 + \tilde{V}, \tag{33}$$

with

$$\tilde{V}(\tilde{x}) = \begin{cases} \frac{1}{2}\tilde{\omega}^2\tilde{x}^2 + \tilde{\lambda}\tilde{x}^4 & \text{if } |\tilde{x}| < 1 \\ \infty & \text{if } |\tilde{x}| \geqslant 1. \end{cases} \tag{34}$$

With these rescalings, $x_{\max}$ has disappeared from the problem and we can now expand $\tilde{E}$ as a double series in $\tilde{\lambda}$ and $\tilde{\omega}$. This can be done using the usual methods of perturbation theory since we can solve the problem exactly when $\tilde{\lambda} = \tilde{\omega} = 0$. The perturbative series becomes

$$\tilde{E}_n = \sum_{k=0,l=0}^{\infty} E_n^{(k,l)} \tilde{\lambda}^k \tilde{\omega}^{2l}, \tag{35}$$

with dimensionless coefficients $E_n^{(k,l)}$. Scaling back to the original problem, we obtain

$$E_n = \sum_{k=0,l=0}^{\infty} E_n^{(k,l)} \lambda^k \omega^{2l} x_{\max}^{6k+4l-2}. \tag{36}$$

Comparing with equation (9), we conclude that with this expansion

$$E_n^{(k)}(\sqrt{\omega}x_{\max}) = \sum_{l=0}^{\infty} E_n^{(k,l)} \times \left(\omega x_{\max}^2\right)^{2l+3k-1}. \tag{37}$$

Obviously, this implies that the asymptotic behaviour when $x_{\max} \to 0$, for the ratios displayed in figure 1, is

$$R_k(\sqrt{\omega}x_{\max}) \propto x_{\max}^{6k-2}. \tag{38}$$

We checked numerically that this asymptotic behaviour is correct. Using the data of figure 1, one can indeed determine the constant of proportionality $E_0^{(l,0)}$ calculated independently below with more than two significant digits.

For the ground state,

$$E_0^{(0,0)} = \frac{\pi^2}{8} \qquad E_0^{(1,0)} = \frac{1}{5} - \frac{4}{\pi^2} + \frac{24}{\pi^4} \qquad E_0^{(0,1)} = \frac{1}{6} - \frac{1}{\pi^2}. \tag{39}$$

Higher orders require infinite sums. In practice, since we see from equation (34) that the calculations can be performed with $x_{\max} = 1$, it is easier to proceed numerically as in section 2 but with a double series. The numerical results are given in table 1 and displayed in figure 7.

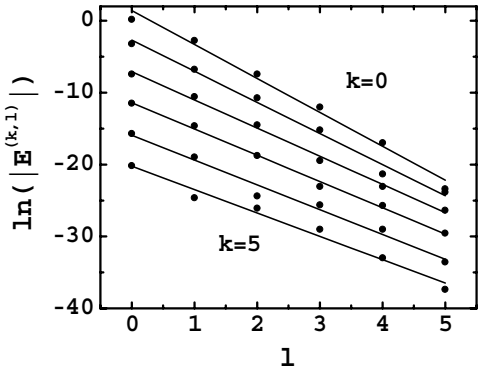

Figure 7. $\ln(|E^{(k,l)}|)$ versus l, the order of expansion in ω^2, for $k = 0, 1, \ldots, 5$. The lines represent linear fits for a given k.

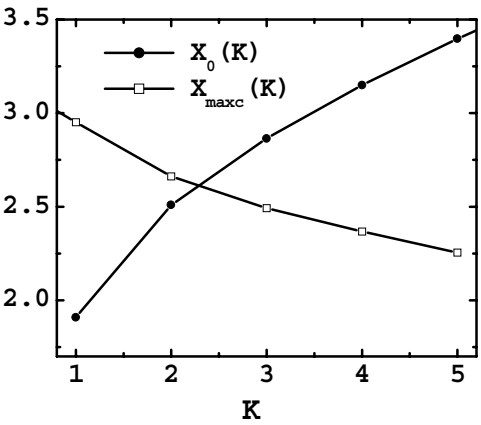

Figure 8. Estimated values of $x_{\max c}(k)$ for which we reach the radius of convergence for $\omega = 1$ (empty boxes) and values of $x_0(k)$ (black circles) where the crossover occurs as defined in section 7, for $k = 1, \ldots, 5$.

The approximately linear behaviour of $\ln\left(\left|E_0^{(k,l)}\right|\right)$ in l at fixed k shown in figure 7 suggests that the power series in $\omega^2 x_{\max}^4$, for the coefficients of $(\lambda/\omega^3)^k$ have a finite radius of convergence (see equation (37)). As the slopes vary from -4.7 for $k = 0$ to -3.3 for $k = 5$, we expect that the series converge for $|x_{\max}\sqrt{\omega}| < \mathrm{e}^{4.7/4} \simeq 3.3$ for $k = 0$ to $\mathrm{e}^{3.3/4} \simeq 2.3$ for $k = 5$. Figure 8 shows a steady decrease of the radius of convergence when k increases. At the same time, the value of $x_{\max}$ where the transition between the small and large cutoff limit occurs, denoted $x_0(k)$ increases with k. This quantity is defined more precisely in section 7. Consequently, it seems clear that as the order increases, a gap opens between the range of validity of the small $x_{\max}$ expansion and the crossover region.

6. Rigorous lower bounds on the radius of convergence

In sections 3 and 5, we have discussed the radius of convergence of series from a numerical point of view. We now return to this question with more analytical considerations. First of all, it is possible to get an order magnitude estimate for the radius of convergence by using a

simple argument. If we look at a typical term of the perturbative series at order λ^k, it is the product of k matrix elements for the perturbation potential x^4 divided by $k-1$ differences of energy level. The matrix elements of x^4 are bounded in magnitude by $x_{\max}^4$. The differences of energy depend on $x_{\max}$. If $x_{\max}$ is very small, in other words if $x_{\max}^2\omega^2 \ll \omega$ in units where the mechanical mass and $\hbar$ are set to 1, the harmonic term is a perturbation and the energy differences are proportional to $x_{\max}^{-2}$. For instance, the difference between the ground state and the first excited state will be approximately $3\pi^2/(8x_{\max}^2)$. In the opposite limit of large $x_{\max}$, the level is approximately equidistant with a separation ω. From this we expect that the perturbative series converges for $|\lambda| < \lambda_c(x_{\max}, \omega)$ with

$$\lambda_c(x_{\max}, \omega) \propto \begin{cases} x_{\max}^{-6} & \text{if } x_{\max} \ll \omega^{-1/2} \\ \omega x_{\max}^{-4} & \text{if } x_{\max} \gg \omega^{-1/2}. \end{cases} \tag{40}$$

This argument does not take into account aspects such as the number of terms present or their signs; however, a rigorous *lower* bound on the radius of convergence can be obtained by simply using one half of the difference between the ground state and the first excited state of the unperturbed system in the above argument. This is formulated precisely in theorem XII.11 in [14] and proved in [15]. The final result in our case is

$$\lambda_c(x_{\max}, \omega) > (1/2)\left(E_1^{(0)} - E_0^{(0)}\right)/x_{\max}^4. \tag{41}$$

Note that theorem XII.11 is more than what we need here because the perturbation is a bounded operator and we do not need to compare its norm with the norm of H_0.

In the case $\omega = 0$, dimensional analysis dictates $\lambda_c(x_{\max}, \omega = 0) = Cx_{\max}^{-6}$ for some positive C, and equation (41) implies

$$\lambda_c(x_{\max}, \omega = 0) > (3\pi^2/16) \times x_{\max}^{-6}. \tag{42}$$

This bound can be compared with numerical estimates obtained from the series with coefficients $E_0^{(k,0)}$ defined in section 5 and which only requires one calculation with $x_{\max} = 1$ instead of the two step procedure of section 3. Using the coefficients for $k = 5, \ldots, 10$, we obtain

$$\lambda_c(x_{\max}, \omega = 0) \simeq 53 \times x_{\max}^{-6}, \tag{43}$$

which is quite close to the result obtained with $\omega = 1$ at low $x_{\max}$ in section 5. The rigorous bound on C, $3\pi^2/16 \simeq 1.85$ is about 30 times smaller than the empirical value 53. In summary, the lower bound is compatible with our numerical estimate, but is not sharp.

The same argument can be applied for the calculation of $E_0^{(0)}$ as a power series in $(1/2)\omega^2$ for the perturbation $(1/2)\omega^2x^2$. It can be tested by studying the coefficients $E^{(0,l)}$ as we did in section 5. The rigorous bound becomes $(1/2)\omega_c^2 > (1/2)(3\pi^2/8)/x_{\max}^4$, which implies

$$\omega_c > 1.92 \times x_{\max}^{-2}. \tag{44}$$

From section 5, we have

$$\omega_c \simeq (3.3)^2 \times x_{\max}^{-2}, \tag{45}$$

and again, the lower bound is compatible with the numerical estimate, but is not an accurate estimator of the actual radius of convergence.

7. The crossover region: empirical data collapse

In this section, we discuss the question of the interpolation between the large and small $x_{\max}$ approximation. In section 4, we have already observed that by naively using integral formulae

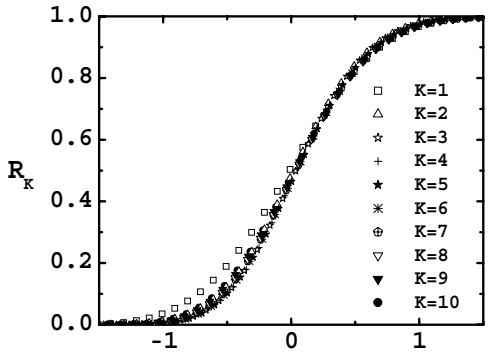

Figure 9. $R_k(x_+x_0(k))$ for $k = 1, \ldots, 10$.

derived in the large $x_{\max}$ approximation for $E^{(0)}$ and $E^{(1)}$, it was possible to obtain decent approximations at low $x_{\max}$. We will first explain how this works and then discuss the higher orders terms.

In the (mathematical) limit of very small $x_{\max}$, equation (23) implies that $G_0(x) \simeq -\omega x^2$. Consequently, in this limit, where we do not expect the approximation to be accurate, the correction becomes dominant and we have

$$E_0^{(0)}(\sqrt{\omega}x_{\max}) \simeq 1\big/\big(\omega x_{\max}^2\big). \tag{46}$$

Despite the lack of justification for this formula, it is not far from the accurate answer derived in section 5:

$$E_0^{(0)}(\sqrt{\omega}x_{\max}) \simeq \pi^2\big/\big(8\omega x_{\max}^2\big) \simeq 1.234\big/\big(\omega x_{\max}^2\big). \tag{47}$$

Similarly for $E^{(1)}$, we can study equation (28) in the mathematical limit of small $x_{\max}$. According to section 4, $\Psi_0^{(0)}(x) \simeq (1 - (x/x_{\max})^2)$ and elementary integration yields

$$E_0^{(1)}(\sqrt{\omega}x_{\max}) \simeq (1/21) \times \big(\omega x_{\max}^2\big)^2 \simeq 0.0476\big(\times\omega x_{\max}^2\big)^2. \tag{48}$$

Again, this is close to the accurate answer from equation (39):

$$E_0^{(1)}(\sqrt{\omega}x_{\max}) \simeq 0.0411 \times \big(\omega x_{\max}^2\big)^2. \tag{49}$$

For higher orders, we know from figure 8 that the small $x_{\max}$ approximation is not convergent in the crossover region. However, the shape similarities observed in figure 1 suggest to parametrize R_k in terms of a single function U that can be shifted by a k-dependent quantity that we denote $x_0(k)$. We have chosen $x_0(k)$ as the value of $x_{\max}$ for which the second derivative of R_k vanishes. The numerical values are shown in table 2 and figure 8. Empirically, it can be fitted quite well with

$$x_0(k) \simeq 0.87 + 1.13\sqrt{k}. \tag{50}$$

In figure 9, we show that the possibility of having

$$R_k(x_{\max}) \simeq U(x_{\max} - x_0(k)), \tag{51}$$

is reasonably well satisfied for $k \geqslant 2$. In other words, with suitable translations, the R_k approximately 'collapse'.

Table 2. $x_0(k)$ for $k = 1, \ldots, 10$.

	$x_0(k)$
1	1.908
2	2.509
3	2.868
4	3.152
5	3.398
6	3.626
7	3.839
8	4.042
9	4.235
10	4.421

8. Conclusions

We have shown that the calculation of the perturbative series for the anharmonic oscillator with a field cutoff $x_{\max}$ can be performed reliably using numerical methods, and approximate analytical methods in the limit of small and large $x_{\max}$. For the coefficients of order 0 and 1 in λ, the integral formulae derived in the large $x_{\max}$ limit, produce the correct leading power dependence with coefficients close to the correct ones, in the opposite limit (small $x_{\max}$) where they are not expected to be accurate. For higher orders, it is possible to approximately collapse the crossover region of the various order by an appropriate translation in $x_{\max}$. The collapse is not perfect and it is necessary to resolve more accurately the details of figure 9 in order to obtain accurate formulae for the R_k.

We expect that it is possible to extend the small and large cutoff techniques in the case of higher dimensional field theory; however the only numerical method that we can envision for the crossover region is the Monte Carlo method [16]. In view of this, it is essential to reach a proper understanding of the interpolation.

Acknowledgments

This research was supported in part by the Department of Energy under Contract No FG02-91ER40664 and in part by the National Science Foundation under Grant No PHY99-07949. This work was completed while YM was visiting the Kavli Institute for Theoretical Physics. YM thanks the organizers and participants of the workshop 'Modern Challenges for Lattice Field Theory' for conversations. We thank J Cook for checking series expansions in section 4 and B Kessler for providing independent checks of the numerical estimates of the radius of convergence.

References

[1] LeGuillou J C and Zinn-Justin J 1990 *Large-Order Behavior of Perturbation Theory* (Amsterdam: North-Holland)
[2] Pernice S and Oleaga G 1998 *Phys. Rev.* D **57** 1144
[3] Meurice Y 2002 *Phys. Rev. Lett.* **88** 141601 (*Preprint* hep-th/0103134)
[4] Bender C M and Boettcher S 1998 *Phys. Rev. Lett.* **80** 5243
[5] Li L and Meurice Y 2005 *Phys. Rev.* D **71** 016008 (*Preprint* hep-lat/0410029)
[6] Kessler B, Li L and Meurice Y 2004 *Phys. Rev.* D **69** 045014 (*Preprint* hep-th/0309022)
[7] Li L and Meurice Y 2005 *Phys. Rev.* D **71** 054509 (*Preprint* hep-lat/0501023)

[8] Buckley I R C, Duncan A and Jones H F 1993 *Phys. Rev.* D **47** 2554
[9] Duncan A and Jones H F 1993 *Phys. Rev.* D **47** 2560
[10] Bender C and Wu T T 1969 *Phys. Rev.* **184** 1231
[11] Meurice Y 2002 *J. Phys. A: Math. Gen.* **35** 8831 (*Preprint* quant-ph/0202047)
[12] Szego G 1939 *Orthogonal Polynomials* (Providence, RI: American Mathematical Society)
[13] Cook J 2004 Private communication
[14] Reed M and Simon B 1978 *Methods of Modern Mathematical Physics: IV Analysis of Operators* (San Diego, CA: Academic)
[15] Kato T 1966 *Perturbation Theory for Linear Operators* (New York: Springer)
[16] Li L and Meurice Y 2004 *Nucl. Phys. Proc. Suppl.* **129** 883 (*Preprint* hep-lat/0309066)